Anisotropy of the Electron and Hole Drift Mobility in KNbO$_3$ and BaTiO$_3$

Pietro Bernasconi, Ivan Biaggio, Marko Zgonik, and Peter Günter

Nonlinear Optics Laboratory, Institute of Quantum Electronics, Swiss Federal Institute of Technology,
ETH Hönggerberg, CH-8093 Zürich, Switzerland

We determine the anisotropy of the mobility of photoexcited charge carriers in single crystals of KNbO$_3$ and BaTiO$_3$ by means of a purely optical method. In orthorhombic KNbO$_3$ the mobility anisotropy is measured for both electrons and holes giving $\mu_a/\mu_c = 1.05 \pm 0.06$, $\mu_b/\mu_c = 2.9 \pm 0.3$ for holes and $\mu_a/\mu_c = 1.15 \pm 0.09$, $\mu_b/\mu_c = 1.9 \pm 0.2$ for electrons. In BaTiO$_3$ we find for holes $\mu_a/\mu_c = 19.6 \pm 0.6$. Our experiment also demonstrates that the acoustic phonon contribution to the dielectric permittivity is substantially different for spatially modulated electric fields as compared to the homogeneous case.   [S0031-9007(96)02051-0]

The drift mobility of photoexcited holes in tetragonal barium titanate (BaTiO$_3$) shows an anisotropy of about a factor of 20 between the two different crystallographic directions. A recent work [1] has pointed out that this anisotropy has the same temperature dependence as the anisotropy of the dielectric permittivity, a fact which lead to speculation upon a possible linear relation between the drift mobilities and the dielectric permittivities. Several hypotheses have been examined trying to explain these phenomena but none was completely satisfactory. The description of the charge transport by small-polaron hopping was not completely successful [1], either, although it was demonstrated that in BaTiO$_3$ this process is dominant [2]. We now present new measurements of the anisotropy of the photoexcited charge carrier mobility in potassium niobate (KNbO$_3$), another anisotropic polar material of the same family and with characteristics similar to those of BaTiO$_3$.

These two materials belong to the oxygen-octahedra ferroelectrics with perovskite structure and are particularly interesting for electro-optical, nonlinear optical as well as for photorefractive applications [3–5]. Although at different temperatures, both crystals have the same sequence of structural phase transitions, from the cubic to the tetragonal, orthorhombic, and finally to the low temperature rhombohedric phase. In the lower symmetry phases, both crystals are ferroelectric and show a spontaneous polarization P_S associated with a weak lattice distortion. At room temperature KNbO$_3$ is orthorhombic (point group $mm2$) with the crystallographic b axis in the pseudocubic [010] direction, while the a and c axes lie along the pseudocubic [101] and [$\bar{1}$01] directions. At room temperature, BaTiO$_3$ has a tetragonal structure (point group 4 mm) with the axes parallel to the cubic ones. In both materials the c axis is oriented parallel to P_S.

We determine the anisotropy of the mobility in the bulk of the material from the photoconductivity measured by a purely optical method. Using light energies smaller than the material band gap, the photoconductivity is due to charge photoexcitation from energy levels introduced by impurities or intentional doping. In contrast to direct photoconductivity measurements, our results are not influenced by the quality of contacts between crystal and electrodes or by parasitic buildup of screening charges close to the electrodes themselves or by surface conductivity, all of which are particularly inconvenient effects in highly insulating materials like KNbO$_3$ and BaTiO$_3$.

We measure the bulk photoconductivity by detecting the decay of the space-charge electric fields generated by the photoconductivity itself. Two interfering laser beams first create a spatially sinusoidal charge carrier excitation rate which leads to a charge displacement from the brighter to the darker regions of the interference pattern. At steady state and small modulation depth of the interference pattern, this process converges to a sinusoidal charge distribution inside the impurity centers [6,7] and the resulting dc electric space-charge field modulates the refractive index of the crystal via the linear electro-optic (Pockels) effect. The amplitude of the generated phase grating is monitored by the diffraction of a weak probe beam incident at the Bragg angle. The diffracted intensity is proportional to the square of the space-charge field amplitude [6,8]. We study the decay of the phase grating when it is erased by a strong homogeneous illumination. By measuring the grating decay times for various orientations of the grating wave vector, we determine the anisotropy of the photoconductivity and thus of the charge mobility.

The amplitude of the space-charge field grating decays exponentially. The exponential time constant τ is given by [5]

$$\tau(I) = \frac{\epsilon^{\text{eff}}\epsilon_0}{e\mu n(I)}\left(\frac{1 + k_g^2/k_D^2}{1 + k_g^2/k_0^2}\right),   (1)$$

where ϵ^{eff} and ϵ_0 are the effective [9] and the vacuum dielectric constants, e is the unit charge, n is the density of free charge carriers with mobility μ, and k_g is the modulus of the grating vector. The Debye screening

wave vector k_0 and the inverse diffusion length k_D are two material constants which depend on the impurity concentration [5]. The density of photocarriers $n(I)$ is responsible for the light intensity dependence of Eq. (1). This formula is valid for sinusoidal modulations of the space-charge distribution obtained by a low contrast illuminating interference pattern.

We choose the magnitude of k_g to be much smaller than both k_0 and k_D. In this limit the term between parentheses on the right hand side of Eq. (1) can be safely neglected. The decay time constant is then directly given by the dielectric relaxation time $(\epsilon^{\text{eff}}\epsilon_0)/(e\mu n)$. Provided that the number density of photoexcited charges $n(I)$ stays constant, we can write the following expression for angular dependence of the decay time constant:

$$\tau(\vartheta) = \tau_{\vartheta=0}\frac{\epsilon^{\text{eff}}(\vartheta)}{\epsilon_c^{\text{eff}}}\frac{\mu_c}{\mu(\vartheta)}, \qquad (2)$$

where ϑ is the angle between the grating wave vector and the c axis of the crystal and $\mu_c/\mu(\vartheta)$ describes the angular dependence of the mobility. In Eq. (2) an effective permittivity ϵ^{eff} must be used because of the sinusoidal spatial modulation of the internal electric field. In such cases ϵ^{eff} is neither the one corresponding to a strain-free (clamped) crystal, nor the one corresponding to a stress-free (unclamped) crystal. The calculation of the effective dielectric constant for a particular direction of the space-charge field has to take into account the piezoelectric contributions generated by the mechanical response of the crystal to the internal sinusoidal electric space-charge field [9].

In general, the mobility can be described by a diagonal second rank tensor [10]. Although the static electric field E is always parallel to the grating wave vector, the drift current is generally not. Only the component of the current density parallel to the grating wave vector is responsible for the decay of the space-charge grating. By calculating this component for every direction of the grating wave vector, we can compute the effective scalar mobility as a function of ϑ. The mobility ratio appearing in Eq. (2) is then given by

$$\frac{\mu(\vartheta)}{\mu_c} = \cos^2(\vartheta) + \frac{\mu_{a,b}}{\mu_c}\sin^2(\vartheta), \qquad (3)$$

where the subscripts a, b, and c denote the axes along which the mobility is considered.

In contrast to previous studies [1,11] where only two extremal points were measured, we determine the full dependence of the decay times τ of the space-charge grating on the angle ϑ between k_g and the c axis. We choose a very large grating period of 45 μm ($k_g = 0.14~\mu$m^{-1}) in order to neglect the terms in the parentheses on the right hand side of Eq. (1). Taking into account that $k_0, k_D > 1.25~\mu$m^{-1}, the error introduced is less than 1%. The measurements have been performed in many different KNbO$_3$ crystals including pure, iron doped, p-type and n-type samples, and in a nominally

pure BaTiO$_3$ probe. The crystals, cut with the surfaces normal to the crystallographic axes, are mounted so that they can be rotated around the surface normal bisecting the directions of the two beams which produce the grating ($I_{\text{w1}} = 0.03$ W/cm^2 and $I_{\text{w2}} = 0.21$ W/cm^2). These two beams and the erasing beam ($I = 3.5$ W/cm^2) are provided by an Ar$^+$ laser operating at 488 nm. All polarizations are always adjusted perpendicular to the c axis to reduce possible beam coupling or beam fanning effects [12]. The monitor beam (He-Ne laser at 633 nm, $I = 0.01$ W/cm^2) is polarized along the c axis. While rotating the samples, we readjust all the polarizations by means of $\lambda/2$ plates in order to ensure the same writing and, in particular, identical erasing conditions. In this way $n(I)$ remains unchanged and independent of ϑ.

After the grating has reached the steady state, the grating decay is induced by blocking the two writing beams and by simultaneously switching on the strong erasing beam. All the decay curves measured for different ϑ follow a single exponential function over at least ten decay time constants. We perform a least-squares fit of the angular dependence of τ using Eq. (2), in which the angular dependence is governed by the single parameter $\mu_{a,b}/\mu_c$. The scaling parameter $\tau(0)$ does not influence the form of the curves; $\epsilon^{\text{eff}}(\vartheta)/\epsilon_{\vartheta=0}^{\text{eff}}$ is known [9,13].

Figure 1 shows the grating decay time vs grating wave vector orientation in the BaTiO$_3$ crystal, while Figs. 2 and 3 present the results for KNbO$_3$. The solid lines correspond to the least squares fit using Eq. (2). The agreement is remarkable. The mobility anisotropies obtained from the fits are summarized in Table I. The measurement performed in the hole conducting BaTiO$_3$ crystal agrees with the value obtained in Refs. [1,11,14]. Experiments in electron conducting samples of BaTiO$_3$ could not be performed because no suitable crystal was
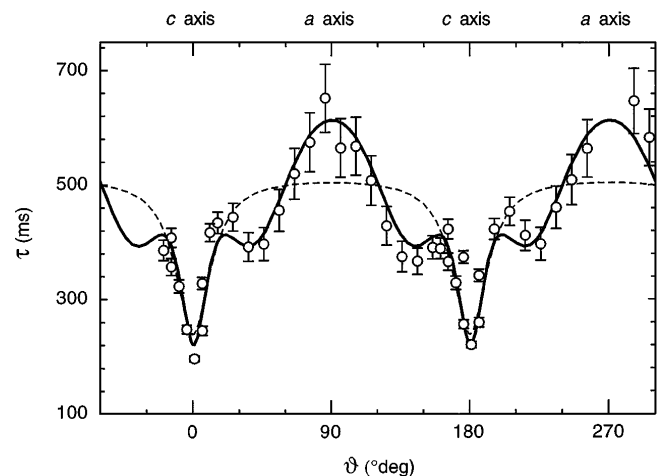

FIG. 1. Decay time of the photoinduced space-charge grating in a nominally pure BaTiO$_3$ crystal as a function of the angle between k_g and the c axis of the crystal. The solid line represents the fit with Eq. (2) using $\epsilon^{\text{eff}}(\vartheta)$. The dashed curve is the fit obtained when using the uncorrected clamped or unclamped dielectric constants.
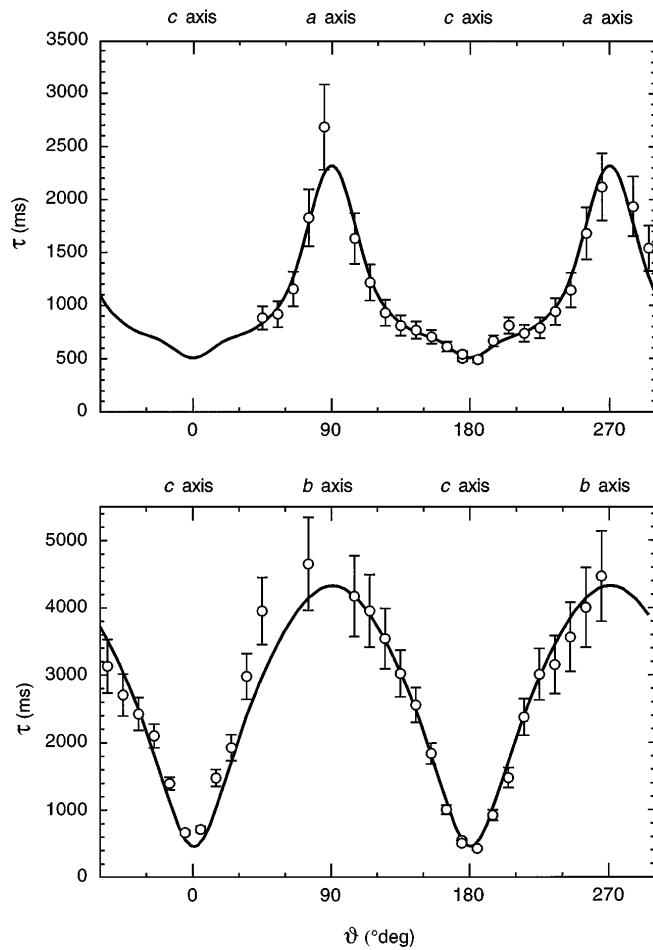
FIG. 2. Decay time of the photoinduced space-charge modulation in an iron doped hole conducting $KNbO_3$ crystal as a function of the angle between k_g and the c axis of the crystal. Angular dependence in the a-c plane (above) and in the b-c plane (below). The solid line represents the fitted curve calculated from Eq. (2).
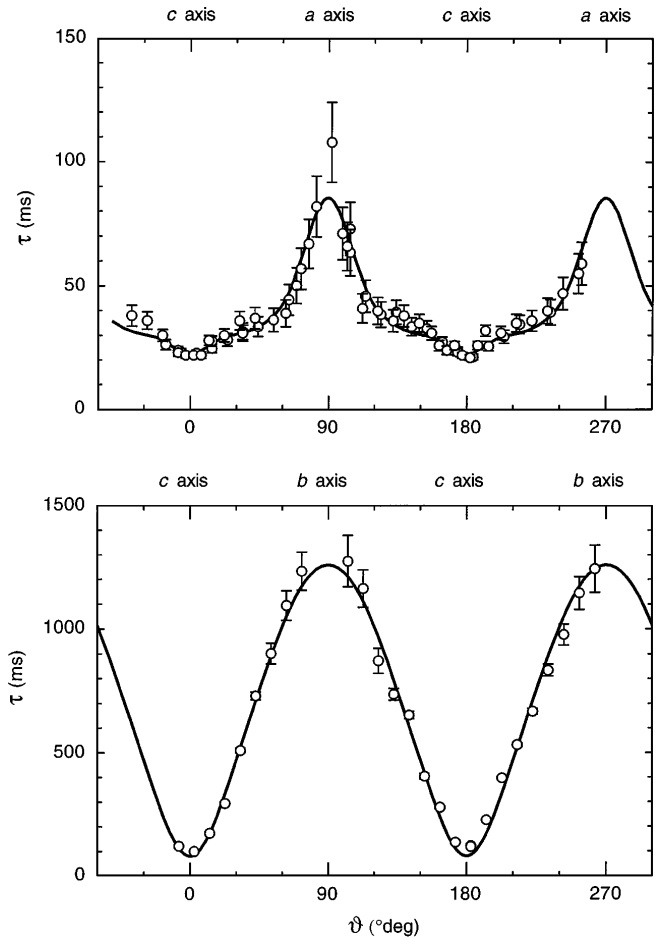

FIG. 3. Decay time of the photoinduced space-charge modulation in an iron doped electron conducting $KNbO_3$ crystal as a function of the angle between k_g and the c axis of the crystal. Angular dependence in the a-c plane (above) and in the b-c plane (below). The solid line represents the fitted curve calculated from Eq. (2).

available. The only previous measurements in $KNbO_3$ have been published in Ref. [15], but they are affected by a poor accuracy [16]. Since the absolute value of the drift band mobility along the c axis for the electrons in $KNbO_3$ is $\mu_c = 0.5 \pm 0.1$ cm^2(Vs)$^{-1}$ [17] we have $\mu_a = 0.6 \pm 0.2$ cm^2(Vs)$^{-1}$ and $\mu_b = 1.0 \pm 0.3$ cm^2(Vs)$^{-1}$. These values are similar to $\mu_c = 0.13 \pm 0.03$ cm^2(Vs)$^{-1}$ and $\mu_a = 1.2 \pm 0.3$ cm^2(Vs)$^{-1}$ found in $BaTiO_3$ by Hall experiments [18]. Unfortunately, no data are available on the absolute hole band mobility for these two materials.

Our measurements lead to several observations. The mobility ratios do not depend appreciably on the doping concentration since a concentration of the trapping centers of the order of 10^{-5} per unit cell can influence the charge density $n(I)$ but not, or only to a negligible extent, the charge carrier mobility. In $KNbO_3$, the mobility ratio μ_a/μ_c for both electrons and holes is very similar and close to unity, while the ratio μ_b/μ_c shows a larger anisotropy. In $BaTiO_3$, μ_a/μ_c is even larger.

The low mobilities observed in both materials can be understood on the basis of a small-polaron model [19]. In the one dimensional case, the small-polaron hopping mobility is of the type [20]

$$\mu = \frac{ea^2 J^2}{\hbar k_B T \sqrt{4 E_A k_B T / \pi}} \exp(E_A/k_B T), \qquad (4)$$

where a is the interatomic distance, E_A is the activation energy, and J is the overlap integral of the electronic wave functions of the adjacent sites. The anisotropy of the overlap integral can be considered as the origin of the mobility anisotropy [21]. For highly localized wave functions, the overlap integral can be assumed to vary exponentially as $J \propto \exp(-a/r_0)$ where r_0 is the localization length. Thus using Eq. (4) we can write

$$\frac{\mu_{a,b}}{\mu_c} = \left(\frac{a_{a,b}}{a_c} \right)^2 \exp[-2(a_{a,b} - a_c)/r_0]. \qquad (5)$$

In $KNbO_3$ the lattice constants along the $a, b,$ and

TABLE I. Photoconductivity type (P.C.), dopant concentration (Nom. pure: Nominally pure), and drift mobility ratios in single crystals of $KNbO_3$ and $BaTiO_3$.

Sample	P.C.	Doping	μ_a/μ_c	μ_b/μ_c
$KNbO_3$	p	Fe: 150 ppm[a]	1.05 ± 0.06	2.9 ± 0.3
	p	Nom. pure	$\cdots$	3.2 ± 0.4
	p	Nom. pure	$\cdots$	2.9 ± 0.3
	n	Fe: 20 ppm[a]	1.15 ± 0.09	1.9 ± 0.2
$BaTiO_3$	p	Nom. pure	19.6 ± 0.6	
	n	Nom. pure[b]	9.2 ± 5.1[c]	

[a]Concentration in Fe/Nb atomic ratio in the crystal.
[b]Reduced in flowing hydrogen [19].
[c]As determined from Hall measurements in Ref. [19].

c axes are $a_a = 5.6896$ Å, $a_b = 3.9692$ Å, and $a_c = 5.7256$ Å which, combined with the mobility ratios, give a polaron localization r_0 between 0.5 and 3.5 Å. These values would be compatible to the small-polaron model. However, this is not the case for $BaTiO_3$ where the polaron localization was calculated to be 0.03 Å [1], which appears to be unphysically small.

In $BaTiO_3$ another puzzling relation was noticed between mobility and dielectric permittivity and Mahgerefteh *et al.* advanced the hypothesis that the two quantities are not independent. In their work they found $\mu_c/\mu_a = R\epsilon_c/\epsilon_a$ where R is a constant close to 2 and temperature independent over the whole tetragonal phase. Our measurements have been carried out at room temperature but the results demonstrate that R has no universality pretence since its values in $KNbO_3$ are close to 4 and 9 for μ_c/μ_a and μ_c/μ_b, respectively.

As already pointed out above, the solid curves in all the figures have been calculated using the *effective* dielectric permittivity which takes into account the piezoelectric as well as the elastic contributions in the case of a sinusoidal space-charge field. To show the importance of using the correct expression for ϵ^{eff}, in Fig. 1 we also plot the curve of Eq. (2) when ϵ^{eff} is calculated from either the clamped or the unclamped values. An evident disagreement with the measured data is obtained. Our measurement of the dielectric relaxation time as a function of the direction of the space-charge field is thus the first direct experimental confirmation of the validity of the expressions for the effective dielectric constant given in Ref. [9].

In conclusion, we have shown that optical methods can provide a reliable tool for the characterization of the charge drift mobility in photoconductive materials. The measurement of the decay time of a photoinduced space-charge fields as a function of the crystal orientation allows the precise determination of the charge carrier drift mobility ratios.

The localization length of the quasifree charge carriers is calculated in $KNbO_3$ according to the small-polaron model. Its value is consistent with the theory, while that obtained for $BaTiO_3$ is too small. A further comparison of the results in $BaTiO_3$ and in electron and hole conducting $KNbO_3$ shows that the value which relates the mobility ratio with the corresponding dielectric permittivity ratio is a material parameter. The explanation of the temperature independence of this parameter noticed in $BaTiO_3$, and the complete description of the charge transport mechanisms in anisotropic polar materials such as $KNbO_3$ and especially $BaTiO_3$, are still open questions.

[1] D. Mahgerefteh, D. Kirillov, R. S. Cudney, G. D. Bacher, R. M. Pierce, and J. Feinberg, Phys. Rev. B **53**, 7094 (1996).
[2] H. Ihrig and D. Hennings, Phys. Rev. B **17**, 4593 (1978), and references therein.
[3] M. E. Lines and A. M. Glass, *Principles and Applications of Ferroelectrics and Related Materials* (Clarendon, Oxford, 1977).
[4] P. Günter, Phys. Rep. **93**, 199 (1982).
[5] *Photorefractive Materials and Their Applications I: Fundamental Phenomena,* edited by P. Günter and J. P. Huignard, Topics in Applied Physics Vol. 61 (Springer-Verlag, Berlin, 1988).
[6] N. V. Kukhtarev, V. B. Markov, S. G. Odulov, M. S. Soskin, and V. L. Vinetskii, Ferroelectrics **22**, 949 (1979).
[7] G. C. Valley and M. B. Klein, Opt. Eng. **22**, 704 (1983).
[8] H. Kogelnik, Bell Syst. Tech. J. **48**, 2909 (1969).
[9] M. Zgonik, P. Bernasconi, M. Duelli, R. Schlesser, P. Günter, M. H. Garrett, D. Rytz, Y. Zhu, and X. Wu, Phys. Rev. B **50**, 5941 (1994).
[10] J. F. Nye, *Physical Properties of Crystals* (Clarendon, Oxford, 1957).
[11] C. P. Tzou, T. Y. Chang, and R. W. Hellwarth, Proc. SPIE Int. Soc. Opt. Eng. **613**, 58 (1986).
[12] G. Montemezzani, A. A. Zozulya, L. Czaia, D Z. Anderson, M. Zgonik, and P. Günter, Phys. Rev. A **52**, 1791 (1995).
[13] M. Zgonik, R. Schlesser, I. Biaggio, E. Voit, J. Tscherry, and P. Günter, J. Appl. Phys. **74**, 1287 (1993).
[14] S. Sochava, K. Buse, and E. Krätzig, Opt. Commun. **98**, 265 (1993).
[15] S. Sochava, K. Buse, and E. Krätzig, Opt. Commun. **105**, 315 (1994).
[16] K. Buse (private communication).
[17] M. Ewart, I. Biaggio, M. Zgonik, and P. Günter, Phys. Rev. B **49**, 5263 (1994).
[18] C. N. Berglund and W. S. Bear, Phys. Rev. **157**, 358 (1967).
[19] D. Emin, Phys. Today **35**, 34 (1982).
[20] D. Emin and A. M. Kirman, Phys. Rev. B **34**, 7278 (1986).
[21] Y. G. Girshberg, E. V. Bursian, and Y. A. Grushevsky, Ferroelectrics **6**, 53 (1973).